Adsorption of 4-chlorophenol from aqueous solutions with nanoparticles decorated on Fe₃O₄@SiO₂-APTMS-SALAL as an efficient magnetically recoverable nanocomposite

Najmeh Amirmahani[a,b], Nosrat O. Mahmoodi[c,*], Mohammad Malakootian[b,d], Abbas Pardakhty[e], Hakimeh Mahdizadeh[f]

[a]Department of Chemistry, University Campus 2, University of Guilan, Rasht, Iran, email: mahan16095@yahoo.com
[b]Environmental Health Engineering Research Center, Kerman University of Medical Sciences, Kerman, Iran
[c]Department of Chemistry, Faculty of Science, University of Guilan, Rasht, Iran, emails: nosmahmoodi@gmail.com/mahmoodi@guilan.ac.ir
[d]Department of Environmental Health, School of Public Health, Kerman University of Medical Sciences, Kerman, Iran,
email: m_malakootian@kmu.ac.ir
[e]Pharmaceutics Research Center, Neuropharmacology Institute, Kerman University of Medical Sciences, Kerman, Iran,
email: drpardakhti@yahoo.com
[f]Department of Environmental Health, School of Public Health, Zarand School of Medical Sciences, Zarand, Iran,
email: H.Mahdizadeh2018@gmail.com

ABSTRACT

The United States Environmental Protection Agency (USEPA) has reported 4-chlorophenol (4-CP) as a priority pollutant. In this study, nanoparticles decorated on Fe₃O₄@SiO₂-Schiff base (Fe₃O₄@SiO₂-APTMS-SALAL) were synthesized to remove 4-CP from aqueous solutions. The Fe₃O₄@SiO₂-APTMS-SALAL nanocomposite (NC) was characterized using field emission scanning electron microscopy, energy dispersive spectroscopy, transmission electron microscopy, Fourier-transform infrared, X-ray diffraction, and vibrating sample magnetometer analyses. Recovery and desorption of 4-CP were investigated in three cycles. GraphPad Prism software was used for data analysis. The removal efficiency of 97% was obtained for the 4-CP in optimum conditions: pH = 7, contact time = 5 min, adsorbent dose: 100 mg/L, and 4-CP initial concentration: 15 mg/L. Studying the kinetic and isotherm equations showed that the process of adsorption followed the second-order kinetics and Freundlich isotherm. The removal rate and adsorption capacity for the real sample were 85% and 127.5 mg/g, respectively. Using Fe₃O₄@SiO₂-APTMS-SALAL NC provided some advantages such as high adsorption capacity (833 mg/g), magnetic reusability of the adsorbent with high activity, mild experimental conditions, and green solvent. Hence, it can be used as an effective adsorbent in water and wastewater treatment.

Keywords: Fe₃O₄@SiO₂-APTMS-SALAL; Nanocomposite; Adsorption; 4-Chlorophenol; Wastewater; Phenolic compounds

1. Introduction

Phenol and its derivatives are natural products that are obtained from the decomposition of plants and animals. Phenolic compounds (PCs) enter the environment in different concentrations from many industries including petrochemical, coal production, rubber manufacturing, paper, plastic, refineries, Fe, steel, Al, leather, and phenolic resins. Almost all PCs are toxic and the carcinogenic nature of some of them has been proven. Further, these compounds cause health problems via entering the human

* Corresponding author.

food chain. 4-CP with the chemical formula of C_6H_5OCl is one of the CPs, in which Cl has replaced H number 4 in the phenol ring [1,2]. World Health Organization (WHO) estimated that one-quarter of all diseases are attributable to environmental pollution [3]. This substance enters the body through the skin, respiration, and digestion and, as a toxic and corrosive chemical, causes irritation and burning of the eyes, skin, nose, as well as coughing and respiratory problems. Long-term contact with this substance causes a headache, fatigue, restlessness, damage to the kidneys and liver, muscle weakness, nausea, and eventually coma and death [4]. The USEPA has introduced phenolic compounds as high-priority contaminants and recommended 1 mg/L inception for these compounds while being discharged into H_2O resources [2,5,6]. Therefore, wastewater contaminated with PCs should be treated before being discharged into the receiving resources. Biological treatment [7], photocatalytic processes [8,9], and electrochemical methods [10] are the most important methods for removing phenol and PCs from wastewater. Problems such as high cost, low efficiency, and production of toxic and hazardous byproducts are the limiting factors in the usage of some of these methods [2,5,11,12]. Among these methods, adsorption by nanostructures is one of the most recommended physicochemical water and wastewater industry treatment processes because of its merits like high efficiency, simple operation, fast response, low cost, and many environmental benefits [6,13].

The disadvantages of adsorbent separation by time-consuming centrifugation and filtration methods are resolved by applying magnetic nano-sorbents. Also, nano-sorbents are easily separated from the media using an external magnetic field [2,14–18]. Owing to the advantages of nanomagnetic adsorbents, many articles have been reported in this regard, some of which are Fe_3O_4@poly(EGDMA@ VIM) microspheres [19], Fe_3O_4@mSiO$_2$@DPDES [20], Fe_3O_4@ SiO$_2$@PAN [21], Apt-MNPs [22], Mnp@YM [23], GO-Fe$_3$O$_4$ hybrids [24], nano-particles of zinc oxide-modified date pits [25,26], polypyrrole-TiO$_2$ composite [27], magnetic MCM-48 nanoporous silica [2], Fe_3O_4-coated nanofibers based on cellulose acetate/chitosan [28], Mg–Al layered double hydroxides/single-walled carbon nanotubes NCs [29], magnetic activated carbon [30] that are used for the adsorption of phenols and PCs from aqueous solutions.

Therefore, these NCs can be used for removing PCs from water resources contaminated through industrial activities. Accordingly, this research aims to determine the removal efficiency (RE) of 4-CP from aqueous solutions by Fe_3O_4@SiO$_2$-APTMS-SALAL NCs as a new magnetic NC and investigate the effect of parameters including pH, contact time, amount of adsorbent, and initial concentration of 4-CP on the adsorption process. The benefits of working with Fe_3O_4@SiO$_2$-APTMS-SALAL through high magnetic power make it easy to separate adsorbent from the reaction medium and reuse it. Furthermore, the high surface area in Fe_3O_4@SiO$_2$-APTMS-SALAL increases adsorption power.

2. Materials and methods

All the materials used in this work were of analytical grade. Solvents with a purity of 99.8% were purchased from Merck-Germany. All the synthetic solutions of this study were prepared by twice distilled-H_2O. The pH of the solution was adjusted using 0.1 N H_2SO_4 and 0.1 N NaOH solutions. Furthermore, to disperse the adsorbent in the solution, a shaker with a constant rate of 200 rpm was used.

2.1. Preparing Fe_3O_4@SiO$_2$-APTMS-SALAL NCs

Fe_3O_4 NPs were prepared using simple chemical coprecipitation. FeCl$_2$·4H$_2$O (5 mmol) and FeCl$_3$·6H$_2$O (10 mmol) in 15 mL of deionized-H_2O (DI-H_2O) were solved and the resulting mixture was degassed using Ar. When the temperature reached 80°C, 30 mL of NH$_4$OH was added to the solution until the pH was adjusted to 11. The resulting mixture was refluxed at 100°C for 1 h. After this period, the obtained Fe_3O_4 black solid was separated by a magnet, washed with DI-H_2O and EtOH for many times, and dried. To synthesize Fe_3O_4@SiO$_2$, Fe_3O_4 NPs (1.0 g) were first diluted with H_2O (50 mL) and stirred for 10 min. Then, tetraethyl orthosilicate (TEOS) (1 mL) diluted in EtOH (20 mL) was added dropwise to this solution and the reaction mixture was continued to react for 24 h at 80°C. The obtained product was collected by magnetic separation, washed, and dried. Fe_3O_4@SiO$_2$ (1 g) was added to 50 mL of EtOH and stirred for 10 min under Ar atmosphere. 3-Aminopropyl trimethoxysilane (APTMS) (2 mmol) was added to the above mixture and heated at 80°C for 8 h. After the reaction completion, the product was collected by magnetic separation, washed, and dried under vacuum. Fe_3O_4@SiO$_2$-APTMS (1 g) and salicylaldehyde (SALAL) (6 mmol) in 50 mL of EtOH were heated at 60°C for 24 h. The NCs were magnetically separated, washed several times with EtOH, and dried under vacuum at 80°C for 6 h [31–33]. The obtained product was collected by magnetic separation, washed, and dried in a vacuum (Fig. 1).

2.2. Adsorbent characterization analysis

Fe_3O_4@SiO$_2$-APTMS-SALAL NCs were characterized by Fourier transform infrared spectroscopy (FT-IR: 6300, Bruker, Billerica, Massachusetts, US), X-ray diffraction (XRD; Philips X-PERT 1710 diffractometer, Netherlands, Almelo) using Co Kα (λ = 1.78897 Å at the voltage of 40 kV and current of 40 mA) analysis, field emission scanning electron microscopy (FESEM) (MIRA3TESCANXMU), energy dispersive spectroscopy (EDS) (TESCAN mira2), transmission electron microscopy (TEM) (Philips CM30), and vibrating sample magnetometer (VSM) (Lake Shore Cryotronics-7404) techniques.

Solvents were distilled before being used. The FT-IR spectra were recorded as KBr pellets (FT-IR 6300 Brucker) and the FESEM assessments were carried out (MIRA3TESCANXMU). The XRD patterns were achieved by Cu-Kα radiation (λ = 1.78897 Å; 40 kV; 40 mA) using a Philips PW 1710 diffractometer. Data were obtained in the 2θ range 3°–80° using the scanning speed of 0.02 s^{-1}. The adsorbent magnetic properties were assessed by a vibrating magnetometer/alternating gradient force magnetometer (Lake Shore Cryotronics-7404). TGA/DTA was done via a thermic analyzer under a total Ar gas flow (level of heat: 10°C min^{-1} ranging 25°C–600°C) (PC Luxx 409-NETZSCH). The inductively coupled plasma (ICP) analysis was carried out using an inductively coupled plasma-optical emission
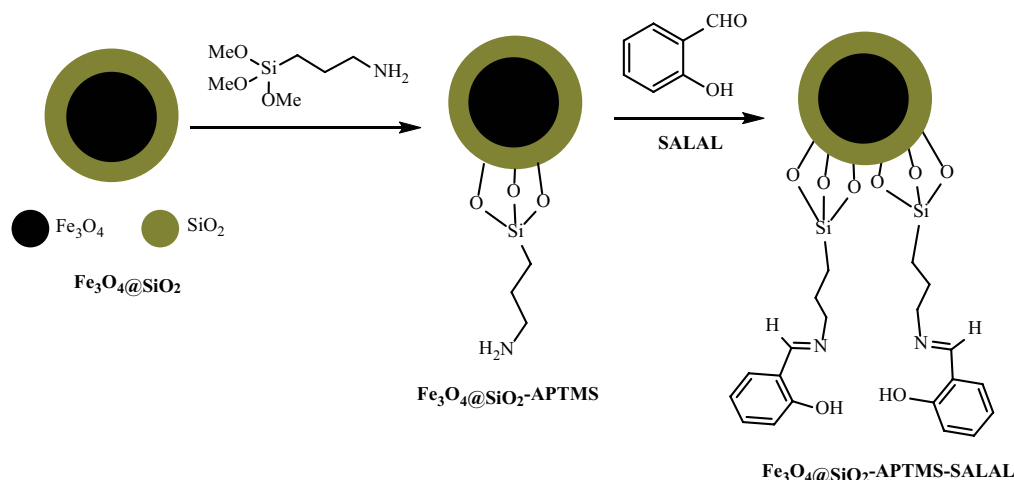
Fig. 1. Synthesis of $Fe_3O_4@SiO_2$-APTMS-SALAL NC.

spectrometer (ICP-OES; ARCOS EOP) and ^{1}H-NMR spectra were recorded by a Bruker INOVA 400 and 300 MHz.

2.3. Adsorption test

To examine the effect and efficiency of each of the factors including pH (3, 5, 7, and 10), contact time (3, 5, 10, 20, and 30 min), adsorbent dose (50, 100, and 150 mg/L), and initial concentration of 4-CP (15, 30, 50, and 80 mg/L) were investigated. Moreover, to obtain the optimal values of each variable, the experiments were performed by varying each influential factor and keeping other factors constant at the optimal value. To enhance the confidence coefficient and accuracy of the experiments, the tests were performed in triplicate. The experiments were performed at the ambient temperature of 25°C and adsorption experiments were performed on the shaker at 200 rpm.

Following adsorption, a specific amount of the solution was withdrawn followed by immediate centrifugation. The residual concentration of soluble 4-CP was determined using high-performance liquid chromatography (YL 9100 Waters, USA) supported by a UV absorbance detector at 280 nm and a C18 HPLC column with a particle size of 5 μm, length of 250 mm, and an internal diameter of 4.6 mm. CH_3CN, AcOH, and DI-H_2O (80:5:15) consisted of the mobile phase. The flow rate of 1 mL/min and 20 μL injections were also considered [34,35].

The equilibrium capacity of adsorption (q_e) represented the amount of 4-CP adsorbed on $Fe_3O_4@SiO_2$-SALAL NC for the synthetic and real solutions, which was calculated by Eq. (1) [6,14].

$$q_e = \frac{(C_0 - C_t)v}{m} \tag{1}$$

where C_0 and C_t denote the concentration of 4-CP in the solution (mg/L) at time = 0 and t, v denotes the solution volume (L), and m is the mass of dried adsorbent added to the bottles (g).

The (RE) of 4-CP in the synthetic and real solutions was calculated by Eq. (2) [6,14]:

$$R = \frac{(C_0 - C_t)}{C_0} \times 100 \tag{2}$$

The experiments were conducted according to the methods explained in Water and Wastewater Standards, Edition 20 [36]. Next, the adsorption isotherms were calculated and the degree of the reaction was determined. The results were analyzed using one-way ANOVA analysis in GraphPad Prism software.

2.4. Recovery process of $Fe_3O_4@SiO_2$-APTMS-SALAL NC

$Fe_3O_4@SiO_2$-APTMS-SALAL NC was recovered through the five consecutive steps after the adsorbent was saturated in the process. 4-CP was recovered under optimum conditions via solvent washing method using MeOH as an extraction solvent. The recovery rate of $Fe_3O_4@SiO_2$-APTMS-SALAL NC was calculated by Eq. (3) [1,37].

$$\%R = \left(\frac{A_t}{A_0}\right)100 \tag{3}$$

where $\%R$ is the recovery rate of $Fe_3O_4@SiO_2$-APTMS-SALAL NC; A_t is the initial concentration of 4-CP (mg/L); A_0 is the desorbed concentration of 4-CP (mg/L).

2.5. Real sample

The real wastewater sample was prepared from the effluent of the coal washing industry. The quality of the real sample was determined and the removal amount of 4-CP was measured under optimal conditions.

3. Results and discussion

3.1. Characterizing $Fe_3O_4@SiO_2$-APTMS-SALAL

FTIR spectrum of $Fe_3O_4@SiO_2$-APTMS-SALAL was studied within the range of 500–4,000 cm^{-1} and the results are shown in Fig. 2.

The absorption band at 3,416 cm^{-1} was attributed to the O–H bonds attached to the surface of silica. The absorption bands at 1,103 and 475 cm^{-1} were attributed to the Si–O and Fe–O bonds, respectively. Aromatic and alkyl C–H stretches were found at 3,073 and 2,895 cm^{-1}, respectively, indicating that the APTMS and SALAL were successfully immobilized on Fe_3O_4 NPs [21,31,32,38].

The expected values for confirming the chemical structure of Fe_3O_4@SiO_2-APTMS-SALAL shown in Fig. 3 were 52.09% O, 21.29% Si, 13.24% Fe, 9.66% C, and 3.72% N in accordance with EDS analysis.

The XRD pattern of Fe_3O_4@SiO_2-APTMS-SALAL NC is presented in Fig. 4. The diffraction peaks of the adsorbent appeared at 2θ of 30.4°, 35.5°, 43.2°, 53.8°, 57.3°, and 63.1°, which were indexed to the diffraction planes of Fe_3O_4 with miller indexes (220), (311), (400), (422), (511), and (440), respectively. All the diffraction peaks contributed to the cubic structure of Fe_3O_4 (JCPDS 75-0033) [32,39,40]. These results confirmed that Fe_3O_4@SiO_2-APTMS-SALAL NC was successfully prepared.

The morphology of the prepared NC was confirmed using FESEM and TEM analyses. As clearly shown in Figs. 5a and b, NC had a well-defined spherical structure.
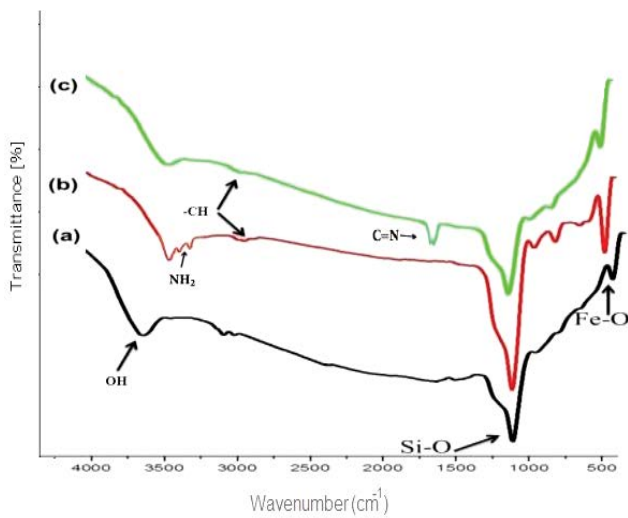
After functionalization with SALAL, Fe_3O_4@SiO_2-APTMS-SALAL maintained their spherical structure, indicating a lack of any morphological changes during the treatment. The particle size was obtained to be about 11–16 nm.

The magnetic properties of Fe_3O_4@SiO_2-APTMS-SALAL NC were evaluated by r. t. VSM (Fig. 6). The magnetization curve of NCs proved a ferromagnetic character. The specific magnetization (M) vs. the applied magnetic field (H) curve indicated the coercive force (H_c), saturation magnetization (M_s), and remnant magnetization (M_r) values for NCs as 0.01 Oe, 14.23, and 0.389 emu/g, respectively. These amounts confirmed enough magnetization power of NCs for simple separation [32,39,41,42].

3.2. Effect of initial 4-CP concentration

The changes in the RE of 4-CP by the Fe_3O_4@SiO_2-APTMS-SALAL at different concentrations of 4-CP (15–80 mg/L), pH = 7, and adsorbent dose of 100 mg/L are presented in Fig. 7.

The results obtained from studying the effect of the initial concentration of 4-CP indicated that, at the constant level of carbon nanotubes, with increasing the initial concentration of 4-CP from 15 to 80 mg/L, the RE dropped from 97% to 84%. This decrease could be attributed to the decrease in the number of available sites for the adsorption of 4-CP with the concentration increase. The optimal concentration of 4-CP was considered in the range of 15 mg/L. With the prolongation of contact time from 5 to 30 min, the
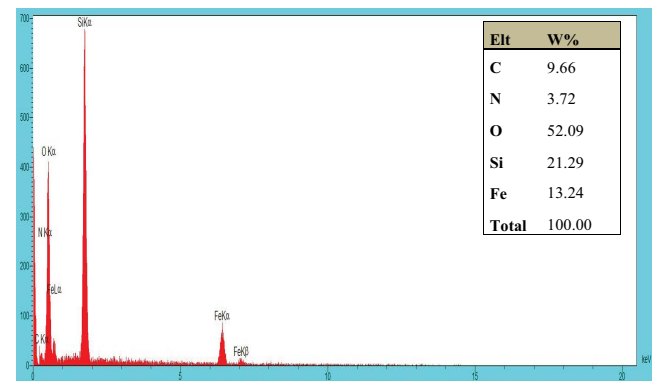

Fig. 2. FT-IR spectra of (a) Fe_3O_4@SiO_2, (b) Fe_3O_4@SiO_2-APTMS, and (c) Fe_3O_4@SiO_2-APTMS-SALAL.

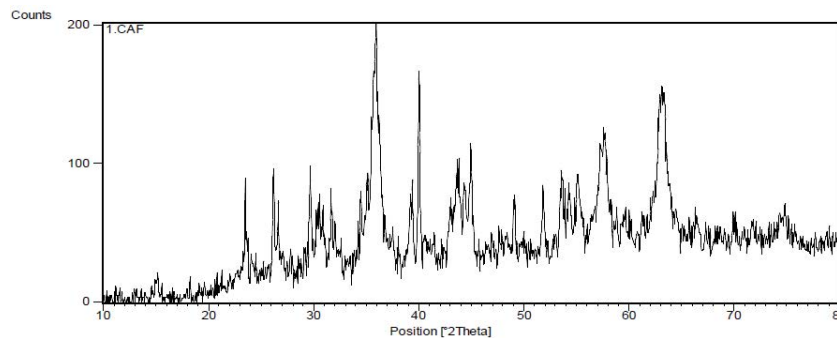| Elt	W%
C	9.66
N	3.72
O	52.09
Si	21.29
Fe	13.24
Total	100.00

Fig. 3. EDS analysis of Fe_3O_4@SiO_2-APTMS-SALAL NC.
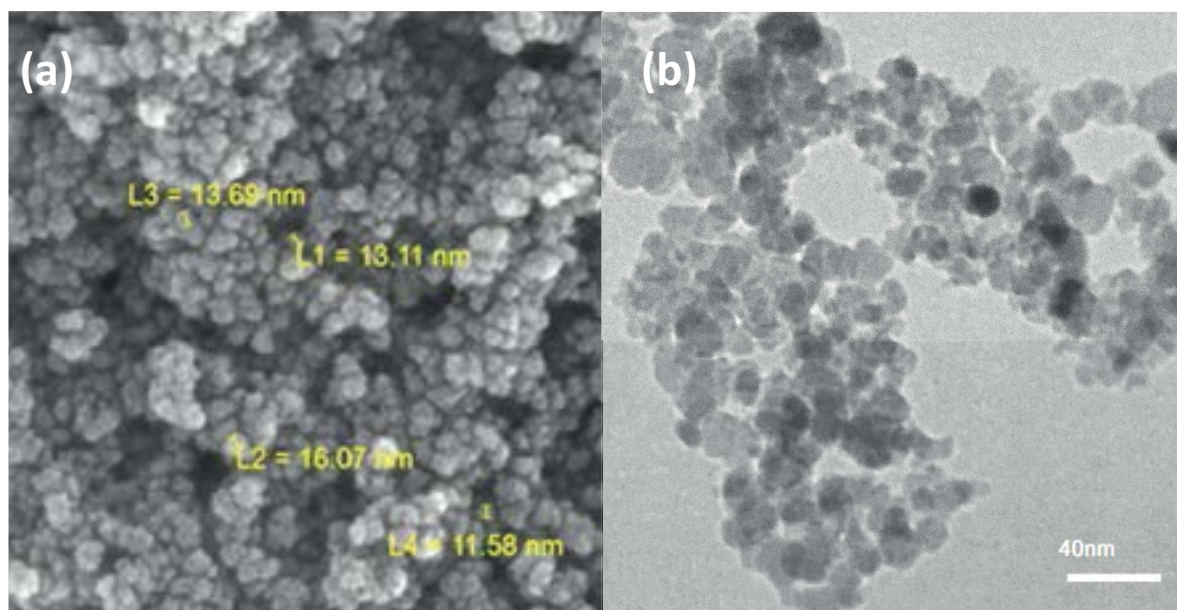

Fig. 4. XRD pattern of Fe_3O_4@SiO_2-APTMS-SALAL NC.

Fig. 5. FESEM (a) and TEM (b) images of Fe_3O_4@SiO_2-APTMS-SALAL NS.

RE declined slowly. As the adsorbent was saturated quickly and with further progress of the process, no change was observed in the RE and even some desorption occurred [9,19]. The ANOVA results showed no significant difference between the initial concentration of 4-CP and the RE ($P > 0.05$).

The results of the study by Malakootian et al. [15] on removing ciprofloxacin antibiotic by $CoFe_2O_4$/activated carbon@chitosan ($CoFe_2O_4$/AC@Ch) indicated that, at pH of 6.5, the temperature of 25°C, and adsorbent level of 0.03 g, with the increase in the concentration of the antibiotic from 10 to 30 mg/L, the RE declined from 93.5% to 59% due to increased repulsion force between the dye molecules. In the study conducted by Noorimotlagh et al. [43], the adsorption mechanism of 4-CP onto activated carbon derived from milk vetch was investigated. Their results confirmed that, with increasing initial 4-CP concentration, the RE of 4-CP decreased due to the limited adsorption sites available for molecule adsorption. The results were consistent with those of other reported studies [29,41].

3.3. Effect of adsorbent dosage

Variations in the RE of 4-CP vs. different concentrations of Fe_3O_4@SiO_2-APTMS-SALAL (50–150 mg/L) with the prolongation of contact time at pH = 7 and 4-CP concentration of 15 mg/L are presented in Fig. 8.

With the increase in the amount of adsorbent from 50 to 100 mg/L, the RE of 4-CP increased from 78% to 97%. This increase was due to the elevated surface of the adsorbent and greater availability for adsorption sites [6,17]. According to one-way ANOVA results, there was a significant difference between the concentration of Fe_3O_4@SiO_2-APTMS-SALAL NC per RE of 4-CP ($P < 0.05$). With a further increase in adsorbent dose from 100 to 150 mg/L, no significant change was observed in the RE. Therefore, 100 mg/L was chosen as the optimal amount of the adsorbent at the optimal time.
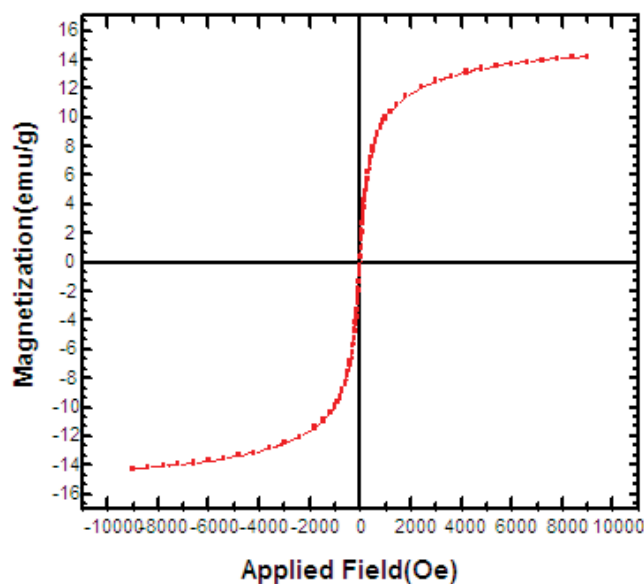

Fig. 6. VSM of Fe_3O_4@SiO_2-APTMS-SALAL NCs.

The results achieved by Zhang et al. [29] on the removal of 4-CP by layered double hydroxides/single-walled carbon nanotubes (CLDH/SWCNT) revealed that, at pH of 6, the contact time of 4 h, and 4-CP concentration of 50 mg/L, with the increase in the amount of the adsorbent from 0. 5 to 0.2 g/L, the RE of 4-CP increased by almost 20%–40%. Malakootian et al. [37] compared the performance of raw multi-walled carbon nanotubes and oxidized multi-walled carbon nanotubes (MWCNTs) in terms of removing *p*-nitroaniline from aqueous solutions and showed that, at the pH of 7, the contact time of 10 min, and initial concentration of 10 mg/L, with the increase in the adsorbent concentration from 0.01 to 0.08 g/100 mL,
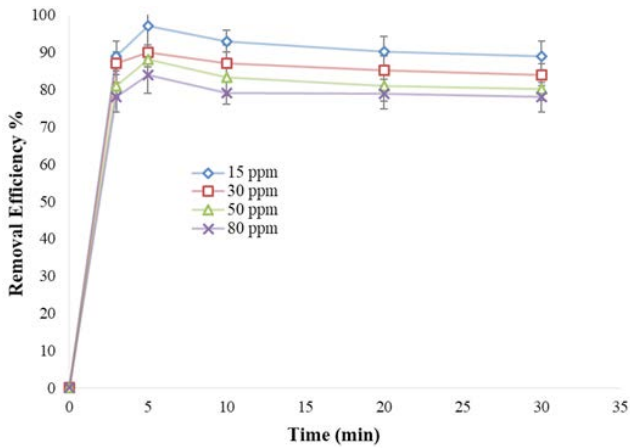
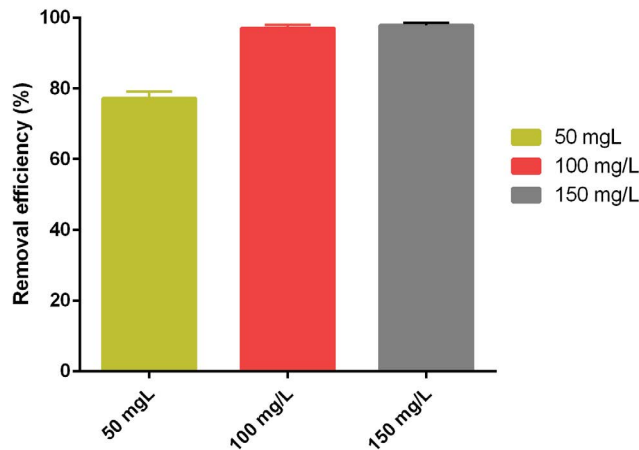Fig. 7. Effect of the initial concentration of 4-CP (adsorbent: 100 mg/L, pH: 7, contact time: 0–30 min).

Fig. 8. Effect of Fe_3O_4@SiO_2-APTMS-SALAL NC concentration (4-CP: 15 mg/L, pH: 7, contact time: 5 min).

the RE increased from 20% and 41% to 73% and 94.8%, respectively. Javid et al. [26] modified carbonized date pits with ZnO nanoparticles and used them as the adsorbent to remove nonylphenol from aqueous solutions. Their results showed that, with increasing the adsorbent dose, the RE of nonylphenol increased. The results of the mentioned studies were in agreement with the results of the present work.

3.4. Effect of initial pH

Changes in the RE of 4-CP with the prolongation of contact time at pH rates of 3, 5, 7, and 10, adsorbent dose of 100 mg/L, and 4-CP concentration of 15 mg/L are demonstrated in Fig. 9.

Solution pH is one of the most important parameters affecting adsorption. The electrostatic interaction between contaminant and adsorbent surface is affected by the pH of the solution. As shown in Fig. 9, the highest RE of CP occurred in an almost acidic to neutral medium (pH: 5–7).

The pH of the solution can change the surface properties of the adsorbent, which corresponded to the pHzpc.
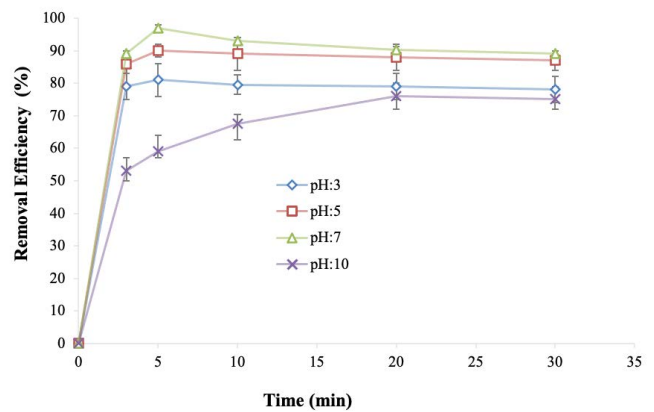

Fig. 9. Effect of initial pH of the solution (adsorption: 100 mg/L, 4-CP: 15 mg/L, contact time: 0–30 min).

On the other hand, with changing the pH of the solution, the surface charge of 4-CP molecules changed according to its pKa [44]. The adsorbent pHzpc using the solid addition method was obtained as 5. At pH > pHzpc, the adsorbent surface was negatively charged, and at pH < pHzpc and neutral pH ≈ pHzpc, the adsorbent surface was positively charged [5].

The pKa of 4-CP was 9.14 at pH above 9.14, 4-CP was ionized to negative ions, and at pH below 9.01, it was ionized to positive ions. Therefore, at pH between 9.14 and 5, the highest adsorption of 4-CP positive ions occurred on the negative surface of the adsorbent [44]. As a result, the electrostatic adsorption of 4-CP on the adsorbent surface increased at these pH ranges. At pH above 9, 4-CP ionized into negative ions; as a result, the electrostatic repulsion between 4-CP molecules and negative adsorbent surface increased and the adsorption efficiency decreased [6,44]. On the other hand, in environments with alkaline pH, the concentration of OH^- in the environment increased, which can inhibit the release of CP ions and, thus, reduce their chances of being absorbed [6,17,44]. Therefore, pH = 7 was selected as the optimum pH. According to the statistical analysis of ANOVA, there was no significant difference in CP RE at different mean pH ($P > 0.05$), which was consistent with the results of other studies. Chen et al. [4] investigated the adsorption behavior of 4-CP and aniline on the adsorbent surface using nanosized activated carbons (NACs). Investigation of the effect of pH on the adsorption efficiency showed that, by increasing pH from 2 to 8, the adsorption efficiency was slightly increased; but, by increasing pH to 10, the adsorption efficiency of 4-CP was significantly decreased due to the electrostatic interaction between the adsorbent surface and 4-CP. In another study by Zhang et al. [29], the absorption rate of 4-CP was measured using layered double hydroxides/single-walled carbon nanotubes (CLDH/SWCNT) and similar results were reported. They found that, at pH below 4 and above 10, the adsorption efficiency of 4-CP decreased due to the change in the surface charge of the adsorbent and the degree of CP ionization in different environments.

In the study conducted by Anbia and Khoshbooei [2] a novel magnetic adsorbent with Fe_3O_4 nanoparticles and melamine-based dendrimer amine functionalized mesoporous silica (MDA–magMCM-48) was prepared and

used for removing CP and bromophenol (BP) from water. Their results confirmed that, at low pH, the amount of adsorption capacity decreased due to the protons presence in water, which competes with CP and BP to be adsorbed on the surfaces of MDA–magMCM-48. The results of the mentioned studies are consistent with the present research findings.

3.5. Contact time effect

The amount of CP adsorbed on Fe_3O_4@SiO_2-APTMS-HBA NC vs. contact time for different concentrations of CP and pH is shown in Figs. 7 and 9. As shown in Fig. 7, at all CP concentrations, the highest amount of CP adsorption occurred in the first 5 min of the process, and the adsorbent was saturated rapidly. With increasing contact time, there was no change in the amount of adsorption and some desorption occurred. In the pH changes diagram, with increasing the contact time under acidic and neutral conditions due to the strong interaction between ionized CP molecules and the adsorbent surface, the highest adsorption occurred at the beginning of the process and, with increasing contact time, the adsorption did not change [28,43].

Under alkaline conditions, the adsorption rate of CP decreased at the beginning of the process, which could be due to the increased competition of CP molecules with hydroxyl ions adsorbed at the adsorbent surfactants [43,44]. With increasing contact time, the CP adsorption increased with a very gentle slope. This may be due to the point that, at alkaline pH, as the contact time of the solution increased, the pH of the solution changed due to the chemical reactions between the dissolved hydroxyl ions and functional groups of the adsorbent surface and decreased to some extent at the end of the reaction [5,44]. Reducing the pH of the solution during the reaction increased the adsorption of CP molecules on the active adsorbent sites.

3.6. Effect of interference of present pollutants in real wastewater samples

Table 1 provides the results of the analysis of the quality of the wastewater of the coal washing industry along with the RE of 4-CP under optimal conditions.

The contaminants' interaction impact in the real wastewater sample was evaluated as well. The existence of soluble and suspended organic materials, sulfate anions, phosphate anions, and other soluble compounds in real wastewater samples competed with 4-CP molecules for adsorption on Fe_3O_4@SiO_2-APTMS-SALAL NC (Table 1). The smaller molecules with a higher propensity in forming bonds with functional groups present on the Fe_3O_4@SiO_2-APTMS-SALAL surface occupied the active points of the nanotube surface [32,39]. Such interfering compounds declined the RE of 4-CP from 97% (synthetic solution) to 85% (real wastewater solution).

3.7. Recovery and desorption of 4-CP on Fe_3O_4@SiO_2-APTMS-SALAL NC

Desorption experiments are important for evaluating the recovery and reusability of adsorbents in water and

Table 1
Analysis results of the quality of the wastewater of coal washing industry and 4-CP removal efficiency

Analysis	Results
pH	5.5
Electrical conductivity (μs/cm)	3,240
Turbidity (NTU)	45
COD (mg/L)	570
BOD_5 (mg/L)	340
TDS (mg/L)	3,700
TSS (mg/L)	210
PO_4^{-3} (mg/L^1)	10
SO_4^{-2} (mg/L)	970
4-CP^a (%)	85%

^{a}Removal efficiency by Fe_3O_4@SiO_2-APTMS-SALAL NC of wastewater at optimum conditions (adsorbent: 100 mg/L, pH: 7, and time: 5 min)

wastewater treatment processes to reduce adsorption costs [1]. Therefore, the desorption tests were conducted in five consecutive cycles using MeOH as the extraction solvent of CP at the concentration of 0.01, 0.05, 0.1, and 0.15 mol/L at the 4-CP minimum and maximum concentrations of 15 and 80 mg/L, respectively, and under optimum conditions of other variables (Fig. 10). The percentage of recovery of 4-CP increased by increasing MeOH concentration from 0.01 to 0.1 mol/L; subsequently, a further increase in MeOH concentration had no effect on recovery rate. By increasing the concentration of 4-CP, the percentage of adsorbent recovery also increased slightly, which might be due to the increased concentration of 4-CP at higher concentrations in addition, Fe_3O_4@SiO_2/APTS retained their magnetic properties during the recovery process and were easily separated from the solution using magnets. The results confirmed that Fe_3O_4@SiO_2-APTMS-SALAL can be recovered and reused by applying the magnetic field; therefore, it can be used in water and wastewater industries to absorb various pollutants from aqueous solutions and even to recover and reuse some valuable pollutants [20].

3.8. Reusability

The reusability of Fe_3O_4@SiO_2-APTMS-SALAL NC for the adsorption of 4-CP was investigated under the optimal conditions of the adsorption process. After the 4-CP adsorption and desorption process, the recycled biocomposite was washed twice with distilled-H_2O and dried at 70°C for 24 h for reuse [5,20]. The RE of 4-CP was determined in four consecutive cycles under optimal desorption process conditions. Based on the obtained results (Table 2), no significant decrease in the RE of 4-CP was observed after three times of reusing.

3.9. Comparing adsorbent performance before and after modification

To evaluate the efficiency of the synthesized adsorbent, the RE of CP was investigated before and after adding functional groups. The results are shown in Fig. 11.

Table 2
Reusability of Fe₃O₄@SiO₂-APTMS-SALAL NC for adsorption of 4-CP
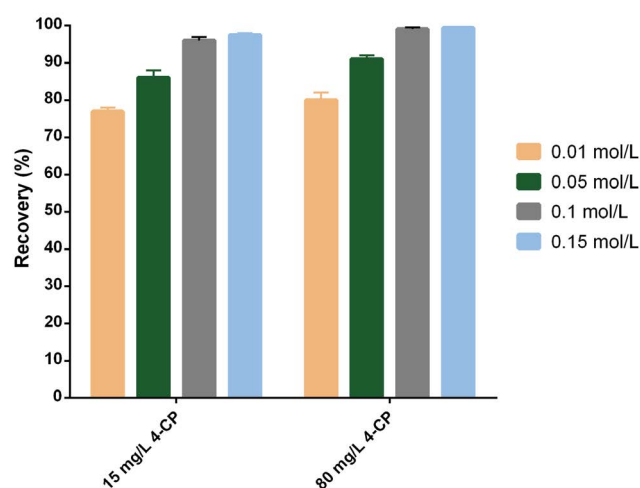
Cycle	Removal efficiency (%)
1	97
2	95
3	94
4	90

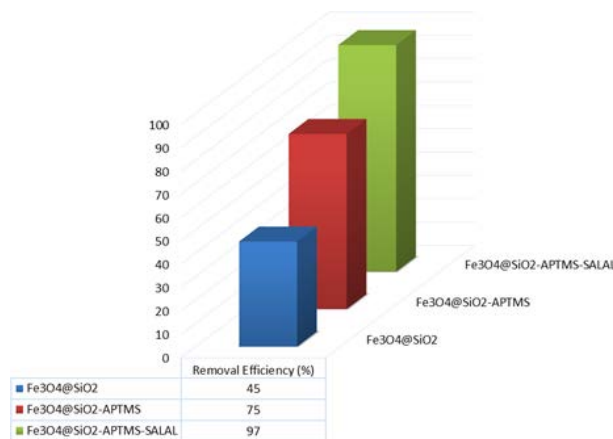Fig. 10. Recovery of 4-CP on Fe₃O₄@SiO₂-APTMS-SALAL NC.

Fig. 11. Comparison of the adsorbent performance before and after modification in 4-CP removal.

Table 3
Parameters of Langmuir and Freundlich isotherms (adsorbent: 100 mg/L, contact time: 5 min, and pH: 7)

Freundlich isotherm			Langmuir isotherm			
R^2	K_f (mg/g) (1/mg)	$1/n$	R^2	R_1	q_m (mg g⁻¹)	K_L (1/mg)
0.98	1.95	0.45	0.88	0.49	833	4.16
				0.008		
				0.005		
				0.003		

Based on the results in Fig. 11 and the FTIR spectra, the RE of 4-CP using the Fe₃O₄@SiO₂ adsorbent increased from 45% to 75% by adding NH₂ and C–H functional groups (Fe₃O₄@SiO₂-APTMS). Using SALAL to add functional groups such as C=N and O–H to the surface NC, the CP RE increased by 97%. The proposed removal mechanism is shown in Fig. 12.

3.10. Isotherm and kinetic models

The constant coefficients and correlation coefficients of the Freundlich and Langmuir adsorption isotherms are provided in Table 3.

The graphs of adsorption isotherms are shown in Figs. 13 and 14.

The adsorption process followed the Freundlich isotherm. The isotherm studies explain how an adsorbate interacts with the adsorbent. Langmuir's theory is based on the assumption that adsorption occurs in a series of special homogeneous sites inside the adsorbent [16,45,46]. Freundlich isotherm is obtained under the assumption of a heterogeneous surface with the non-uniform distribution of the adsorption heat on the surface [16,45,46]. The obtained results (Table 3) indicated that the adsorption process followed the Freundlich isotherm ($R^2 = 0.98$).

A comparison between the q_m of adsorbents in the previously reported literature and the present study is shown in Table 4.

As shown in Table 4, the maximum equilibrium adsorption capacity of the synthesized Fe₃O₄@SiO₂-APTMS-SALAL NC was much higher than that of the other adsorbents, indicating high adsorption capacity.

A comparison between adsorbent q_m in the previously reported literature and the present study is shown in Table 4. Adsorption as a physiochemical process involves the mass transfer of the adsorbate from the solution phase to the adsorbent surface. Several kinetic models are used to analyze such reactions plus the transfer behavior of the adsorbate molecules. First- and second-order kinetic models are known as the used models [16,45,46].

The kinetics of 4-CP removal process by Fe₃O₄@SiO₂-APTMS-SALAL was also examined. The graphs of adsorption kinetics are shown in Figs. 15 and 16.

In the first-order kinetic study, the equilibrium capacity of adsorption (q_e) was found to be 1.9 mg/g, R^2 (correlation coefficient) was found as 0.315, and K_1 (the rate constant) was found as 0.088 min⁻¹. In the second-order kinetics, q_e, R^2, and K_2 were obtained to be 137 mg/g, 0.9993, and 0.00005 (g/mg min), respectively. Based on the obtained results, the process followed second-order kinetics.

According to the adsorption capacity, the first-order kinetic equation is employed in the cases, where adsorption is done with diffusion via a boundary. The second-order kinetic equation, according to adsorption of the solid phase, shows that chemical adsorption is done at the phases with a slower adsorption rate managing the adsorption processes [16,45,46]. The second-order reaction
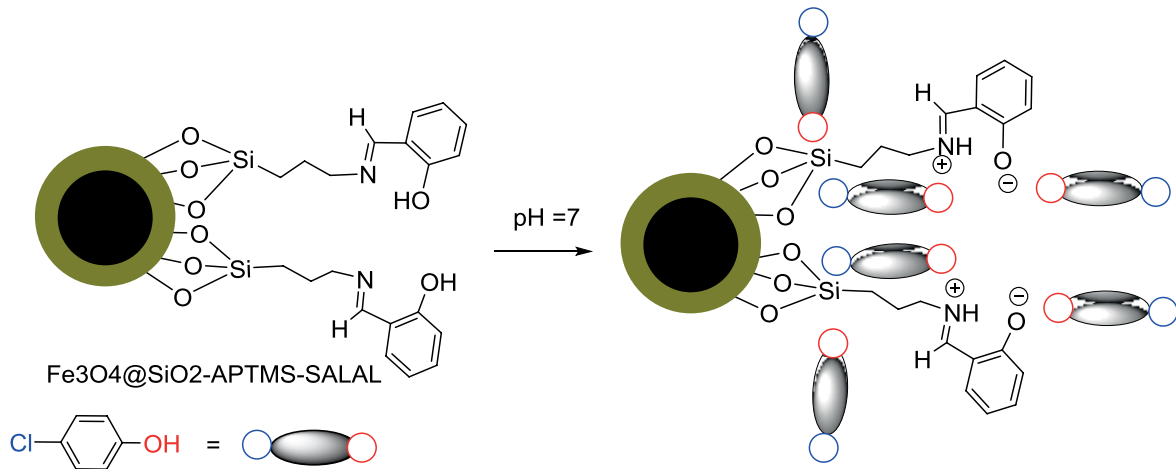
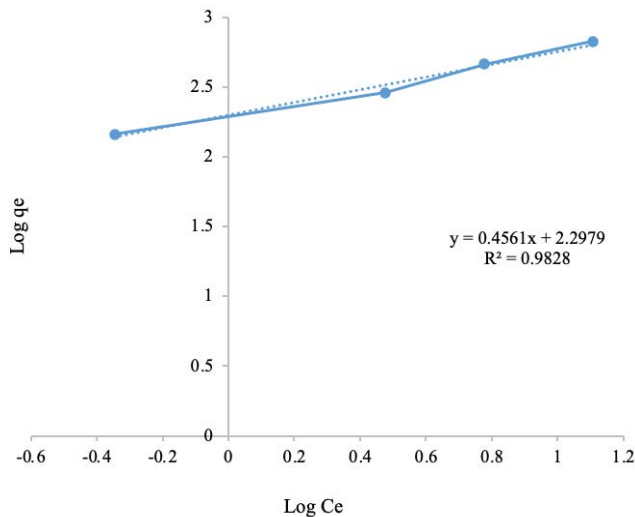Fig. 12. Proposed mechanism for removing 4-CP at pH = 7 by NC.

Fig. 13. Freundlich isotherm.

Fig. 14. Langmuir isotherm.

Fig. 15. First-order kinetics.

progresses at a rate proportional to the second power of a precursor. In second-order kinetics, two reactions are possible. A reaction occurs promptly reaching the equilibrium, whereas the other is slow and can be continued for a long period [16,45,46]. In this study, the primary adsorption rate was high with a very rapid adsorption process (5 min). Following these 5 mins, however, the adsorption process continued at a lower rate. The expressed correlation coefficients demonstrated that the adsorption process followed the second-order kinetics.

3.11. Comparing CP adsorption with other studies

The adsorption of 4-CP and the optimal conditions in this study were compared with previous studies. The results are shown in Table 5.

As shown in Table 5, in comparison with 4-CP removal studies, the contact time in this study was much shorter than that of other studies. In adsorption processes, equilibrium time is one of the most important operating parameters, which also has a great impact on economic
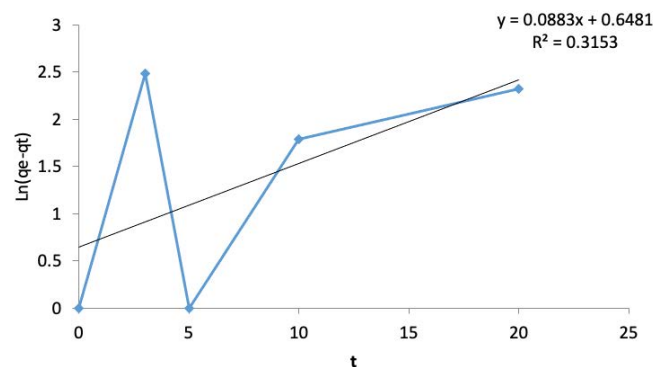
costs. Therefore, a short adsorption equilibrium time can help reduce process costs. Also, in this study, the amount of adsorbent used was much lower than that in the reported studies and the highest amount of 4-CP adsorption was done in the lowest amount of adsorbent dose. In adsorption processes, the synthesis of nanoparticles is one of the

Table 4
Comparison between the q_m of adsorbents

Entry	Adsorbent	Pollutant	q_m	Ref.
1	Fe_3O_4@poly(EGDMA@VIM)	Phenol	33.83	[19]
2	Fe_3O_4@mSiO_2@DPDES	Bisphenol A	120.2	[41]
3	Ordered mesoporous carbon (CMK-3)	4-CP	333	[47]
4	Multiple-walled carbon nanotubes (MWCNT)	4-CP	133	[47]
5	Single-walled carbon nanotubes (SWCNT)	4-CP	58.8	[47]
6	Carbon nanofiber (CNF)	4-CP	111	[47]
7	Nano carbon (NC)	4-CP	142.86	[47]
8	Graphene	4-CP	125	[47]
9	Fe_3O_4@SiO_2-APTMS-SALAL	4-CP	833	This research

Table 5
Comparing 4-CP adsorption capacity and its optimal conditions

Entry	Adsorbate	Adsorbent	Optimal condition	q_m (mg/g) or/and removal efficiency (%)	Ref.
1	4-CP	Magnetic MCM-48 nanoporous silica	Contact time = 4 h, agitation speed = 250 rpm, adsorbent dosage = 0.2 g/L, ambient temperature = 25°C, initial concentration = 50 mg/L	239.5 mg/g	[3]
2	4-CP	Activated carbon prepared from peanut husk	Contact time = 400 min, pH: 6, adsorbent dosage = 0.7 g/L, ambient temperature, initial concentration = 100 mg/L	89.4 mg/g	[48]
3	4-CP	Azolla filiculoides biomass	Contact time = 75 min, agitation speed = 180 rpm, pH: 5, adsorbent dosage = 10 g/L, ambient temperature = 25°C, initial concentration = 10 mg/L	75%	[46]
4	4-CP	Activated carbon synthesized from aloe vera green wastes	Contact time = 40 min, agitation speed = 200 rpm, pH: 2, adsorbent dosage = 3 g/L, ambient temperature = 25°C, initial concentration = 20 mg/L	47 mg/g	[6]
5	4-CP	Activated carbon prepared from rattan sawdust	Contact time = 24 h, agitation speed = 120 rpm, pH: acidic, adsorbent dosage = 0.2 g/L, temperature = 28°C, initial concentration = 100 mg/L	188 mg/g 80%	[14]
6	4-CP	Fe_3O_4@SiO_2-APTMS-SALAL	Contact time = 5 min, agitation speed = 120 rpm, pH: 7, adsorbent dosage = 0.1 g/L, temperature = 25°C, initial concentration = 15 mg/L	833 mg/g 97%	This research

main stages of the process. The time of synthesis and consumption of chemicals are very important. Therefore, adsorbents that have the highest adsorption capacity at their lowest concentration can be suitable adsorbents to replace other adsorbents. In all of these reported studies, the highest adsorption of 4-CP has occurred at acidic to neutral pH rates, which is consistent with the present study.

4. Conclusion

Fe_3O_4@SiO_2-APTMS-SALAL NC has a high potential for removing compounds including heavy metals, organic compounds, carcinogenic compounds, aromatic compounds, etc. The results of this research indicated that Fe_3O_4@SiO_2-APTMS-SALAL with high adsorption capacity (q_m: 833 mg/g) can remove toxic 4-CP with an efficiency
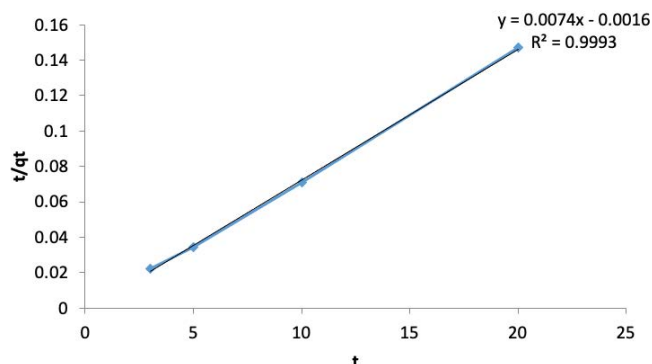
Fig. 16. Second-order kinetics.

of 85% from real wastewater within 5 min. Therefore, it can be used in the water and wastewater industry for removing toxic and hazardous contaminants within a short period of time. In this process, the greatest removal occurred at a pH of 7 and a concentration of 100 mg/L for the carbon nanotubes.

Acknowledgments

References

[1] B. Kakavandi, M. Jahangiri-rad, M. Rafiee, A.R. Esfahani, A.A. Babaei, Development of response surface methodology for optimization of phenol and p-chlorophenol adsorption on magnetic recoverable carbon, Microporous Mesoporous Mater., 231 (2016) 192–206.

[2] M. Anbia, S. Khoshbooei, Functionalized magnetic MCM-48 nanoporous silica by cyanuric chloride for removal of chlorophenol and bromophenol from aqueous media, J. Nanostruct. Chem., 5 (2015) 139–146.

[3] M. Malakootian, Z. Darabi-Fard, N. Amirmahani, A. Nasiri, Evaluation of arsenic, copper, lead, cadmium, and iron concentration in drinking water resources of central and Southern Bardsir Plain, Iran, in 2014, J. Kerman Univ. Med. Sci., 22 (2015) 542–554.

[4] C. Chen, X. Geng, W. Huang, Adsorption of 4-chlorophenol and aniline by nanosized activated carbons, Chem. Eng. J., 327 (2017) 941–952.

[5] H.M. Marwani, E.M. Bakhsh, Selective adsorption of 4-chlorophenol based on silica-ionic liquid composite developed by sol–gel process, Chem. Eng. J., 326 (2017) 794–802.

[6] Y. Omidi-Khaniabadi, A. Jafari, H. Nourmoradi, F. Taheri, S. Saeedi, Adsorption of 4-chlorophenol from aqueous solution using activated carbon synthesized from aloe vera green wastes, J. Adv. Environ. Health Res., 3 (2015) 120–129.

[7] J. Zhao, X. Chen, L. Bao, Z. Bao, Y. He, Y. Zhang, J. Li, Correlation between microbial diversity and toxicity of sludge treating synthetic wastewater containing 4-chlorophenol in sequencing batch reactors, Chemosphere, 153 (2016) 138–145.

[8] X. Zhao, P. Wu, M. Liu, D. Lu, J. Ming, C. Li, J. Ding, Q. Yan, P. Fang, Y_2O_3 modified TiO_2 nanosheets enhanced the photocatalytic removal of 4-chlorophenol and Cr(VI) in sun light, Appl. Surf. Sci., 410 (2017) 134–144.

[9] F.J.A. Villaluz, M.D.G. De Luna, J.I. Colades, S. Garcia-Segura, M.-C. Lu, Removal of 4-chlorophenol by visible-light photocatalysis using ammonium iron(II) sulfate-doped nano-titania, Process Saf. Environ. Prot., 125 (2019) 121–128.

[10] R. Nazari, L. Rajic, Y. Xue, W. Zhou, A.N. Alshawabkeh, Degradation of 4-chlorophenol in aqueous solution by sono-electro-Fenton process, Int. J. Electrochem. Sci., 13 (2018) 9214–9230.

[11] K. Rajabizadeh, G. Yazdanpanah, S. Dowlatshahi, M. Malakootian, Photooxidation process efficiency (UV/O_3) for P-nitroaniline removal from aqueous solutions, Ozone: Sci. Eng., 42 (2020) 420–427.

[12] M. Malakootian, M. Khatami, H. Mahdizadeh, A. Nasiri, M. Amiri Gharaghani, A study on the photocatalytic degradation of p-nitroaniline on glass plates by thermo-immobilized ZnO nanoparticle, Inorg. Nano-Metal. Chem., 50 (2020) 124–135.

[13] B.H. Hameed, L.H. Chin, S. Rengaraj, Adsorption of 4-chlorophenol onto activated carbon prepared from rattan sawdust, Desalination, 225 (2008) 185–198.

[14] N. Amirmahani, H. Mahdizadeh, M. Malakootian, A. Pardakhty, N.O. Mahmoodi, Evaluating nanoparticles decorated on Fe_3O_4@SiO_2-Schiff Base (Fe_3O_4@SiO_2-APTMS-HBA) in adsorption of ciprofloxacin from aqueous environments, J. Inorg. Organomet. Polym. Mater., 30 (2020) 3540–3551.

[15] M. Malakootian, A. Nasiri, H. Mahdizadeh, Preparation of $CoFe_2O_4$/activated carbon@chitosan as a new magnetic nanobiocomposite for adsorption of ciprofloxacin in aqueous solutions, Water Sci. Technol., 78 (2018) 2158–2170.

[16] M. Malakootian, A. Nasiri, A. Asadipour, M. Faraji, E. Kargar, A facile and green method for synthesis of $ZnFe_2O_4$@CMC as a new magnetic nanophotocatalyst for ciprofloxacin removal from aqueous media, MethodsX, 6 (2019) 1575–1580.

[17] Z. Duan, W. Zhang, M. Lu, Z. Shao, W. Huang, J. Li, Y. Li, J. Mo, Y. Li, C. Chen, Magnetic Fe_3O_4/activated carbon for combined adsorption and Fenton oxidation of 4-chlorophenol, Carbon, 167 (2020) 351–363.

[18] N. Amirmahani, M. Rashidi, N.O. Mahmoodi, Synthetic application of gold complexes on magnetic supports, Appl. Organomet. Chem., 34 (2020) e5626 (1–19), doi: 10.1002/aoc.5626.

[19] I. Ozdemir, N. Tekin, A. Kara, Magnetic porous polymer microspheres: synthesis, characterization and adsorption performance for the removal of phenol, J. Macromol. Sci., Part A Pure Appl. Chem., 56 (2019) 564–576.

[20] Y. Jia, E. Li, Z. Du, J. Li, F. Cheng, Recovery of bisphenol A by pH-triggered magnetic nanoparticles, Nano, 14 (2019) 1950052 (1–20), doi: 10.1142/S1793292019500656.

[21] M. Iqbal, J. Shah, M.R. Jan, M. Zeeshan, Mixed hemimicelles dispersive solid phase extraction using polyaniline coated magnetic nanoparticles for chlorophenols from water samples, J. Inorg. Organomet. Polym. Mater., 30 (2020) 1430–1437.

[22] Y. Su, C. Shao, X. Huang, J. Qi, R. Ge, H. Guan, Z. Lin, Extraction and detection of bisphenol A in human serum and urine by aptamer-functionalized magnetic nanoparticles, Anal. Bioanal. Chem., 410 (2018) 1885–1891.

[23] D.F. Mercado, P. Caregnato, L.S. Villata, M.C. Gonzalez, Ilex paraguariensis extract-coated magnetite nanoparticles: a sustainable nano-adsorbent and antioxidant, J. Inorg. Organomet. Polym. Mater., 28 (2018) 519–527.

[24] P. Badhai, S. Kashyap, S.K. Behera, Adsorption of phenol red onto GO-Fe_3O_4 hybrids in aqueous media, Environ. Nanotechnol. Monit. Manage., 13 (2020), doi: 10.1016/j.enmm.2019.100282.

[25] N. Javid, M. Malakootian, Removal of bisphenol A from aqueous solutions by modified-carbonized date pits by ZnO nano-particles, Desal. Water Treat., 95 (2017) 144–151.

[26] N. Javid, A. Nasiri, M. Malakootian, Removal of nonylphenol from aqueous solutions using carbonized date pits modified with ZnO nanoparticles, Desal. Water Treat., 141 (2019) 140–148.

[27] S. Silvestri, T.A.L. Burgo, C. Dias-Ferreira, J.A. Labrincha, D.M. Tobaldi, Polypyrrole-TiO_2 composite for removal of 4-chlorophenol and diclofenac, React. Funct. Polym., 146 (2020) 100282, doi: 10.1016/j.reactfunctpolym.2019.104401.

[28] A. Karamipour, P.K. Parsi, P. Zahedi, S.M.A. Moosavian, Using Fe_3O_4-coated nanofibers based on cellulose acetate/chitosan for adsorption of Cr(VI), Ni(II) and phenol from aqueous solutions, Int. J. Biol. Macromol., 154 (2020) 1132–1139.

[29] Z. Zhang, D. Sun, G. Li, B. Zhang, B. Zhang, S. Qiu, Y. Li, T. Wu, Calcined products of Mg–Al layered double hydroxides/single-walled carbon nanotubes nanocomposites for expeditious removal of phenol and 4-chlorophenol from aqueous solutions, Colloids Surf., A, 565 (2019) 143–153.

[30] Y. Rong, R. Han, Adsorption of p-chlorophenol and p-nitrophenol in single and binary systems from solution using magnetic activated carbon, Korean J. Chem. Eng., 36 (2019) 942–953.

[31] M. Ahmadiazar, M. Mamaghani, Synthesis of (2-iminomethyl) pyridine moiety supported on hydroxyapatite-encapsulated-γ-Fe$_2$O$_3$ as an inorganic-organic hybrid magnetic nanocatalyst for the synthesis of thiazole derivatives under ultrasonic irradiation, Curr. Org. Chem., 22 (2018) 1326–1334.

[32] M. Sheykhan, L. Ma'mani, A. Ebrahimi, A. Heydari, Sulfamic acid heterogenized on hydroxyapatite-encapsulated γ-Fe$_2$O$_3$ nanoparticles as a magnetic green interphase catalyst, J. Mol. Catal. A: Chem., 335 (2011) 253–261.

[33] N. Amirmahani, N.O. Mahmoodi, M. Malakootian, A. Pardakhty, N. Seyedi, Pd nanoparticles supported on Fe$_3$O$_4$@SiO$_2$-Schiff base as an efficient magnetically recoverable nanocatalyst for Suzuki–Miyaura coupling reaction, Res. Chem. Intermed., 46 (2020) 4595–4609.

[34] W. Xiang, R. Qu, X. Wang, Z. Wang, M. Bin-Jumah, A.A. Allam, F. Zho, Z. Huo, Removal of 4-chlorophenol, bisphenol A and nonylphenol mixtures by aqueous chlorination and formation of coupling products, Chem. Eng. J., 402 (2020) 126140, doi: 10.1016/j.cej.2020.126140.

[35] L. Xu, J. Wang, Magnetic nanoscaled Fe$_3$O$_4$/CeO$_2$ composite as an efficient Fenton-like heterogeneous catalyst for degradation of 4-chlorophenol, Environ. Sci. Technol., 46 (2012) 10145–10153.

[36] E.W. Rice, R.B. Baird, A.D. Eaton, L.S. Clesceri, Standard Methods in Examination of Water and Wastewater, 22nd ed., American Public Health Association, USA, 2012.

[37] M. Malakootian, M.H. Ehrampoush, H. Mahdizadeh, A. Golpayegani, Comparison studies of raw and oxidized multi-walled carbon nanotubes H$_2$SO$_4$/HNO$_3$ to remove p-nitroaniline from aqueous solution, J. Water Chem. Technol., 40 (2018) 327–333.

[38] F. Tamaddon, A. Nasiri, G. Yazdanpanah, Photocatalytic degradation of ciprofloxacin using CuFe$_2$O$_4$@methyl cellulose-based magnetic nano biocomposites, MethodsX, 7 (2020) 74–81.

[39] L. Lai, Q. Xie, L. Chi, W. Gu, D. Wu, Adsorption of phosphate from water by easily separable Fe$_3$O$_4$@SiO$_2$ core/shell magnetic nanoparticles functionalized with hydrous lanthanum oxide, J. Colloid Interface Sci., 465 (2016) 76–82.

[40] N. Amirmahani, N.O. Mahmoodi, M. Bahramnejad, N. Seyedi, Recent developments of metallic nanoparticles and their catalytic activity in organic reactions, J. Chin. Chem. Soc., 67 (2020) 1326–1337.

[41] M. Malakootian, A. Nasiri, H. Mahdizadeh, Metronidazole adsorption on CoFe$_2$O$_4$/activated carbon@chitosan as a new magnetic biocomposite: modelling, analysis, and optimization by response surface methodology, Desal. Water Treat., 164 (2019) 215–227.

[42] A. Nasiri, F. Tamaddon, M.H. Mosslemin, M. Faraji, A microwave assisted method to synthesize nanoCoFe$_2$O$_4$@methyl cellulose as a novel metal-organic framework for antibiotic degradation, MethodsX, 6 (2019) 1557–1563.

[43] Z. Noorimotlagh, S. Shahriyar, R. Darvishi Cheshmeh Soltani, R. Tajik, Optimized adsorption of 4-chlorophenol onto activated carbon derived from milk vetch utilizing response surface methodology, Desal. Water Treat., 57 (2016) 14213–14226.

[44] G. Mihoc, R. Ianos, C. Pacurariu, Adsorption of phenol and p-chlorophenol from aqueous solutions by magnetic nanopowder, Water Sci. Technol., 69 (2014) 385–591.

[45] B.H. Hameed, Equilibrium and kinetics studies of 2,4,6-trichlorophenol adsorption onto activated clay, Colloids Surf., A, 307 (2007) 45–52.

[46] M.A. Zazouli, D. Balarak, Y. Mahdavi, Application of azolla for 2-chlorophenol and 4-chroropphenol removal from aqueous solutions, Iran. J. Health Sci., 1 (2013) 43–55.

[47] S. Madannejad, A. Rashidi, S. Sadeghhassani, F. Shemirani, E. Ghasemy, Removal of 4-chlorophenol from water using different carbon nanostructures: a comparison study, J. Mol. Liq., 249 (2018) 877–885.

[48] Y. Hu, Y. Rong, S. Li, C. Ji, R. Han, Adsorption of 4-Chlorophenol from Solution by Activated Carbon Prepared from Peanut Husk, Asia-Pacific Engineering and Technology Conference (APETC), 2017.